

Study of Φ -OTDR Stability for Dynamic Strain Measurement in Piezoelectric Vibration

Meiqi REN, Ping LU, Liang CHEN, and Xiaoyi BAO*

Department of Physics, University of Ottawa, Ottawa, ON, K1S5G5, Canada

*Corresponding author: Xiaoyi BAO E-mail: xbao@uottawa.ca

Abstract: In a phase-sensitive optical-time domain reflectometry (Φ -OTDR) system, the challenge for dynamic strain measurement lies in large intensity fluctuations from trace to trace. The intensity fluctuation caused by stochastic characteristics of Rayleigh backscattering sets detection limit for the minimum strength of vibration measurement and causes the large measurement uncertainty. Thus, a trace-to-trace correlation coefficient is introduced to quantify intensity fluctuation of Φ -OTDR traces and stability of the sensor system theoretically and experimentally. A novel approach of measuring dynamic strain induced by various driving voltages of lead zirconate titanate (PZT) in Φ -OTDR is also demonstrated. Piezoelectric vibration signals are evaluated through analyzing peak values of fast Fourier transform spectra at the fundamental frequency and high-order harmonics based on Bessel functions. High trace-to-trace correlation coefficients varying from 0.824 to 0.967 among 100 measurements are obtained in experimental results, showing the good stability of our sensor system, as well as small uncertainty of measured peak values.

Keywords: Optical fiber sensors; phase-sensitive optical time domain reflectometry (OTDR); vibration

Citation: Meiqi REN, Ping LU, Liang CHEN, and Xiaoyi BAO, "Study of Φ -OTDR Stability for Dynamic Strain Measurement in Piezoelectric Vibration," *Photonic Sensors*, 2016, 6(3): 199–208.

1. Introduction

Distributed optical fiber sensors (DOFSs) based on detection and analysis of backscattered light have attracted significant research attention over the past two decades since they provide many advantages over conventional sensors. The distributed static measurements such as temperature or strain sensing have been extensively demonstrated with Brillouin-based DOFSs and optical frequency domain reflectometry (OFDR) [1–3]. However, as for distributed vibration sensing, the measurable frequency response is limited in above schemes because they require to measure the spectral shift continuously and average 10 times – 100 times in

order to increase signal to noise ratio [4, 5]. Phase-sensitive optical time domain reflectometry (Φ -OTDR) is one of promising DOFSs to detect the dynamic disturbances along the fiber. The principle of the Φ -OTDR is based on the interference between Rayleigh backscattered lights from different scattering centers along the fiber within a pulse width. The relative phase changes of the electric fields from scattering centers are highly sensitive to the disturbances at a certain position. Thus, the Φ -OTDR was successfully detection scheme [6, 7]. The long-range Φ -OTDR for intrusion sensing is demonstrated with the assistance of Raman amplification [8]. The Φ -OTDR was also demonstrated for vibration sensing by adopting

Received: 20 April 2016 / Revised: 30 May 2016

© The Author(s) 2016. This article is published with open access at Springerlink.com

DOI: 10.1007/s13320-016-0334-8

Article type: Regular

heterodyne coherent detection [9]. The wavelet denoising method was also introduced in the Φ -OTDR to get a better performance with 50-cm spatial resolution [10]. The high frequency measurement was achieved by combining a Mach-Zehnder interferometer and a Φ -OTDR system [11].

The aforementioned works demonstrated the vibration measurements with frequencies ranging from Hz to kHz in terms of different applications. Although quantifying the vibration is important in some situations such as oil and gas exploration and crack damage detection in structural health monitoring, it was rarely discussed in literature. Several techniques have been demonstrated in Φ -OTDR for quantitative vibration [12] and dynamic strain measurement [13] based on measuring the phase differences between two adjacent sections. However, the challenge for dynamic strain measurements lies in the stochastic feature of Φ -OTDR traces, causing the signal fading and large measurement uncertainty [14–16]. Thus, minimizing intensity fluctuation by optimizing the Φ -OTDR system is necessary for precise dynamic strain measurements in Φ -OTDR.

In this paper, we demonstrate an approach for monitoring the dynamic strain induced by sinusoidal piezoelectric vibration signals. The trace-to-trace correlation coefficient is introduced to study the intensity fluctuation of Φ -OTDR traces, evaluate the stability of the sensor system and measurement uncertainty through standard deviation among 100 vibration measurements. Through the introduction to the trace to trace correlation coefficient, we find an important parameter F , which simulates the strength of phase fluctuation, and we link it to the repeatability of the dynamic strain measurement. With our proposed method, the quantitative vibration signal in a certain range determined by the first order Bessel function is identified by monitoring the peak value of fundamental frequency in the fast Fourier transform

(FFT) spectra.

2. Operation principle

The Φ -OTDR can be used in vibration measurements by distinguishing changes in speckle-like traces of Rayleigh backscattered light. Vibration positions along the sensing fiber can be extracted by subtracting the trace sequences, and vibration frequency can be obtained by performing the FFT on the time domain waveform at each vibration location. The Rayleigh backscattered light in a single-mode fiber can be modeled as a sequential series of spatially discrete reflectors. When a pulse of highly coherent light with a central frequency of f_0 is injected into the sensing fiber, the electric field of the Rayleigh backscattered light at the fiber incident end ($z = 0$) at time τ is the sum of the electric field of every Rayleigh scattering centers over half of the pulse duration from $\tau v_g/2 - w$ to $\tau v_g/2$, which can be expressed as

$$E_{\tau, z=0} = E_0 \sum_{z_j=(\tau v_g - w)/2}^{\tau v_g/2} r_j e^{i(2\pi f_0 \tau + \varphi_j + \delta\varphi_j)} e^{-2\alpha z_j} \quad (1)$$

where E_0 is the initial electric field amplitude, v_g is the group velocity, w is the spatial length of the pulse width, and α is the attenuation coefficient of the fiber. The subscript j represents the j th reflector, and r_j is the reflectance. $\varphi_j = 2\beta z_j$ is the phase where β is the propagation constant. $\delta\varphi_j$ is the time-dependent phase perturbation caused by internal instability of the Φ -OTDR system. External vibration will cause an extra phase change $\varphi_{\text{vib}}(t)$ of the detected signal, and the output intensity can be written as [17]

$$I = \sum_{j=1}^N (E_0 r_j)^2 e^{-4\alpha z_j} + 2 \sum_{j=1}^{N-1} \sum_{k=j+1}^N E_0^2 r_j r_k e^{-2\alpha(z_j+z_k)} \cos(\Phi_{jk} + \delta\Phi_{jk} + \varphi_{\text{vib}}(t)) \quad (2)$$

where $\Phi_{jk} = \varphi_j - \varphi_k$ and $\delta\Phi_{jk} = \delta\varphi_j - \delta\varphi_k$ are respectively the differences between phases of two backscattered signals from j th and k th reflectors, being part of a total number of N Rayleigh

scattering centers within the spatial length of a short pulse.

As the cosine voltage is applied to the cylinder lead zirconate titanate (PZT) where a section of sensing fiber is wrapped around, the fiber length as well as the corresponding modal index and birefringence will experience periodic changes because of piezoelectric effect of piezo ceramics. So the phase change induced by the PZT can be written as

$$\varphi_{\text{vib}}(t) = \frac{2\pi nL}{\lambda} \eta V_m \sin(2\pi f_{\text{vib}} t) \quad (3)$$

where λ is the wavelength of the light source, n is the refractive index of the optical fiber, L is the fiber length wrapped around the PZT, η is the sensitivity coefficient, and V_m is the vibration amplitude. It is indicated that the phase change $\varphi_{\text{vib}}(t)$ is proportional to $V_m \sin(2\pi f_{\text{vib}} t)$. By inserting $\varphi_{\text{vib}}(t)$ into (2) and ignoring the DC-term, the intensity of the Φ -OTDR is an interference signal determined by the AC-term:

$$\begin{aligned} I &\approx 2 \sum_{j=1}^{N-1} \sum_{k=j+1}^N E_0^2 r_j r_k e^{-2\alpha(z_j+z_k)} \cos(\Phi_0 + \varphi_{\text{vib}}(t)) \\ &= 2 \sum_{j=1}^{N-1} \sum_{k=j+1}^N \Gamma E_0^2 r_j r_k e^{-2\alpha(z_j+z_k)} \begin{bmatrix} \cos(\Phi_0) \cos(V_m \sin(2\pi f_{\text{vib}} t)) \\ -\sin(\Phi_0) \sin(V_m \sin(2\pi f_{\text{vib}} t)) \end{bmatrix} \end{aligned} \quad (4)$$

where $\Phi_0 = \Phi_{jk} + \delta\Phi_{jk}$ is a random variable, and Γ is the converting factor which is related to the material and size of PZT itself. Equation (4) can be further

expanded by using an infinite series of Bessel functions:

$$\begin{aligned} I &= 2 \sum_{j=1}^{N-1} \sum_{k=j+1}^N \Gamma E_0^2 r_j r_k e^{-2\alpha(z_j+z_k)} \\ &\quad \left\{ \begin{aligned} &\cos(\Phi_0) \left[J_0(V_m) + 2 \sum_{n=0}^{\infty} J_{2n}(V_m) \cos(2n \cdot 2\pi f_{\text{vib}} t) \right] \\ &-\sin(\Phi_0) \left[2 \sum_{n=0}^{\infty} J_{2n+1}(V_m) \sin((2n+1) \cdot 2\pi f_{\text{vib}} t) \right] \end{aligned} \right\} \\ &= 2 \sum_{j=1}^{N-1} \sum_{k=j+1}^N \Gamma E_0^2 r_j r_k e^{-2\alpha(z_j+z_k)} \\ &\quad \left[\begin{aligned} &J_0(V_m) \cos(\Phi_0) + \\ &J_1(V_m) \cos(\Phi_0 + 2\pi f_{\text{vib}} t) - J_1(V_m) \cos(\Phi_0 - 2\pi f_{\text{vib}} t) + \\ &J_2(V_m) \cos(\Phi_0 + 2\pi \cdot 2f_{\text{vib}} t) + J_2(V_m) \cos(\Phi_0 - 2\pi \cdot 2f_{\text{vib}} t) + \\ &J_3(V_m) \cos(\Phi_0 + 2\pi \cdot 3f_{\text{vib}} t) - J_3(V_m) \cos(\Phi_0 - 2\pi \cdot 3f_{\text{vib}} t) + \dots \end{aligned} \right] \end{aligned} \quad (5)$$

From (5), the output intensity contains sinusoidal signal components with frequencies f_{vib} , $2f_{\text{vib}}$, $3f_{\text{vib}}$, ... and amplitudes relative to $J_1(V_m)$, $J_2(V_m)$, $J_3(V_m)$, ..., and P_{vib} is the peak value of the FFT spectrum at the vibration frequency f_{vib} . P_{vib} is proportional to the vibration amplitude V_m in a certain range which is determined by the first order Bessel function, thus, V_m can be extracted from the P_{vib} measurement.

3. Φ -OTDR system stability analysis

In Φ -OTDR, system noise is attributed to

underlying phase fluctuations originating from various noise sources such as laser frequency drift, phase noise, and thermal noise in electrical and polarization dependence of optical components, and thermal noise in the sensing fiber. The phase fluctuations due to the system noise contribute to intensity fluctuations of Φ -OTDR time domain traces, leading to instability of the sensor system, which can be quantized by an uncertainty of the measured P_{vib} . Thus, analyzing the system stability of Φ -OTDR is important for vibration measurements.

It is noted that the irregular vibrations often occur in nature where they can be decomposed into a multitude of frequency components with unequal cycles. For instance, a piezoelectric transducer tube is often used to generate a single-frequency vibration; however, an imperfect fiber wrapping process can induce non-uniform vibration responses of the sensing fiber. These additional random vibration components may cause an extra phase change $\delta\varphi_{\text{vib}}$ of the detected signal beyond the system noise, contributing to the uncertainty in P_{vib} .

In order to analyze the stability of Φ -OTDR, a trace-to-trace correlation coefficient $R(M)$ is

introduced to quantify the intensity fluctuation of Φ -OTDR time domain traces as well as the standard deviation of the measured P_{vib} , which is defined as

$$R(M) = \frac{1}{M-1} \sum_{i=1}^{M-1} c[k_i(z), k_{i+1}(z)] \quad (6)$$

where c is the correlation function between two adjacent Φ -OTDR traces, M is the total number of traces, and $k_i(z)$ is the normalized intensity of the i th trace at the position z . The correlation coefficient describes similarity between two time domain traces. If both traces are identical, the correlation coefficient is 1.

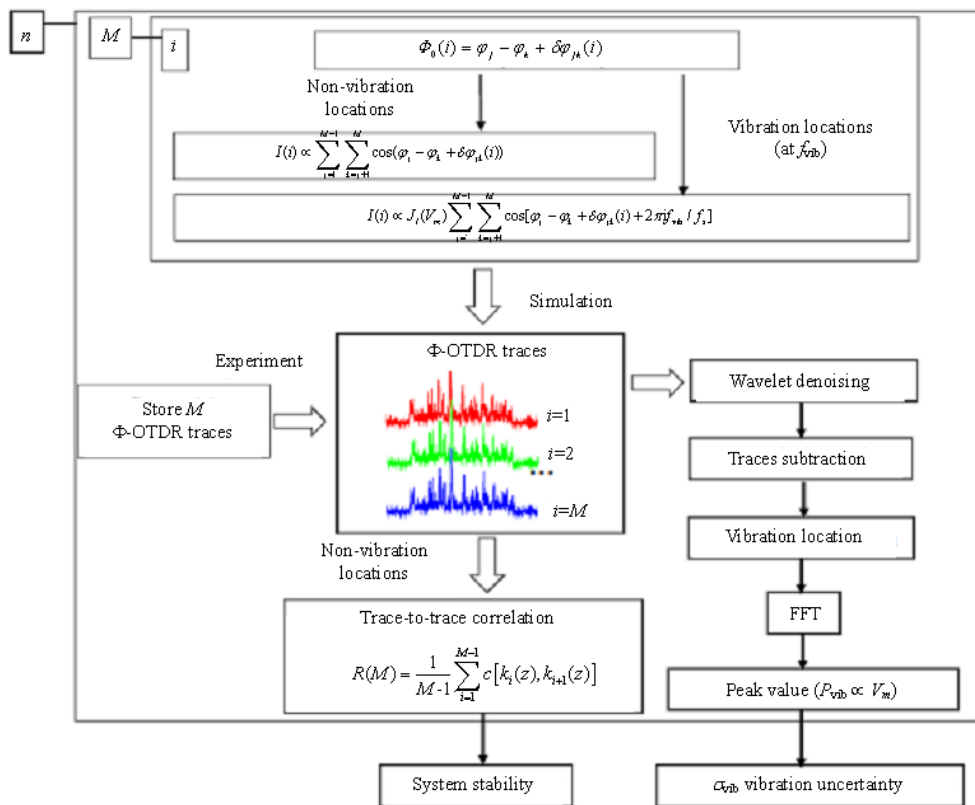


Fig. 1 Flow chart of vibration measurement by using Φ -OTDR.

The system stability is analyzed by calculating R in order to compare with experimental results. The simulation procedure is described in the flow chart of vibration measurement in Φ -OTDR as shown in Fig. 1. In simulation, phase φ of the individual reflector is a random quantity with a uniform

probability distribution over the range of $[0, 2\pi]$. The phase fluctuation $\delta\Phi_{jk}$ has the uniform distribution on $F \cdot [0, 2\pi]$, where the coefficient F has a specific value in the range $[0, 1]$. F factor is used to simulate the strength of phase fluctuations which contribute to intensity fluctuations, and it depends

on the noise in the Φ -OTDR system. Figure 2 shows simulated trace-to-trace correlation coefficients under different F values based on (6) by using 1000 traces. The simulation result illustrates that R decreases monotonically with increasing F . The larger F value is associated with larger phase fluctuation induced by (1) the laser phase noise; (2) local birefringence of the optical fiber, and both of factors will introduce the fluctuation between different traces. For a given fiber, the 2nd contribution is small and fixed; the only variable is the laser phase noise induced time dependent changes. If the laser is phase locked which has slow time variable in phase, the F factor tends to be small, and hence the trace to trace correlation R will remain high as expected, which will allow for the small error in dynamic strain measurement. To get the stable output for the vibration amplitude measurement, which is a relative measurement, it is important to keep low F value and high R value. The minimum F sets the limit for the measureable phase change due to the dynamic strain. This can only happen when the laser phase noise has slow time dependence and birefringence of the fiber is small, and this assumption is valid for all of the single mode fiber with weak Rayleigh backscattering.

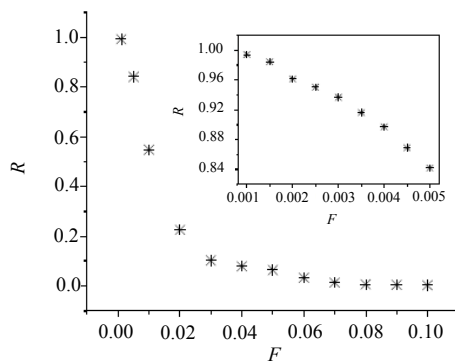


Fig. 2 Simulation results of R as a function of F .

In the experiment, Φ -OTDR traces are acquired and stored in the computer as illustrated in Fig. 1. In order to analyze the system stability, trace-to-trace correlation function is performed at non-vibration locations. The wavelet denoising technique is

adopted in the signal post-processing to reduce the random noise, and then the vibration location can be identified by doing traces subtraction. After obtaining the vibration location, the FFT can be performed along traces at the vibration location, and P_{vib} will be recorded. The experiment will be carried out for n times, and the standard deviation σ_{vib} of the measured P_{vib} is also calculated to quantify the measurement uncertainty.

The experimental setup of the Φ -OTDR system is shown in Fig. 3. An external cavity laser source operated at 1550 nm with a narrow line width of 50 kHz is launched into an electro-optic modulator (EOM) controlled by a function generator to generate optical pulses with a repetition rate of 10 kHz and a pulse width of 50 ns. The EOM bias voltage is locked at the minimum point of the transfer function by utilizing a bias controller with a feedback circuit to maintain the high extinction ratio of the optical pulse. The modulated light is amplified by an erbium-doped fiber amplifier (EDFA1) and then sent into a 675 m sensing fiber (Corning, SMF-28e) via a circulator. The Rayleigh backscattered signals are further amplified through EDFA2, and the amplified spontaneous emission (ASE) noise is filtered out by an optical bandpass filter. Then the signals are measured by a photo-detector (PD) and processed by a data acquisition (DAQ) card.

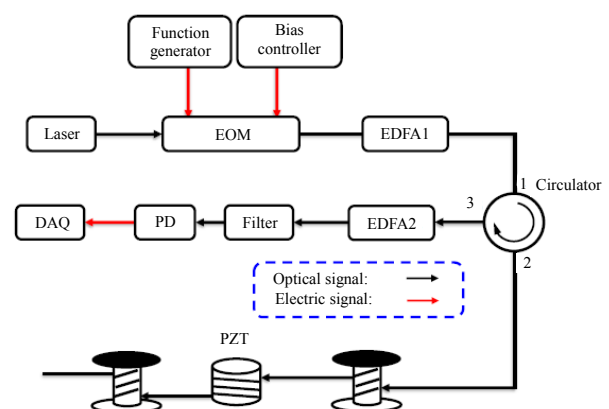


Fig. 3 Experimental setup of the Φ -OTDR system for vibration amplitude measurement.

In the vibration measurement experiment, a section of the sensing fiber is wrapped around a PZT cylinder, and this piezoelectric transducer is driven by a function generator with an output voltage ranging from 0 V to 20 V and a frequency ranging from several Hz up to several kHz.

100 vibration measurements are carried out ($n=100$) to test the system stability. Consecutive Φ -OTDR raw traces ($M = 1000$) in one measurement are experimentally obtained, and the first two adjacent traces as well as the last trace are shown in Fig. 4(a). The corresponding intensity fluctuation at non-vibration locations caused by the noise effects can be characterized by calculating R based on (6). Figure 4(b) shows two traces correlation coefficients $R(2)$ in one experiment. The values are calculated between the first trace and i th

trace, where i is from 2 to 1000. The length of data used is from the starting point to the end point except for the vibration region, labeled in Fig. 4(a). The correlation coefficients $R(2)$ randomly varies from 0.824 to 0.967. The average correlation coefficient $R(1000)$ for one measurement is 0.902, corresponding to a simulated R value when $F \approx 0.004$, as indicated in the inset of Fig. 2. Figure 4(c) shows a histogram distribution with a bin size of 0.01 of calculated correlation coefficients at non-vibration locations for a set of 100 measurements where the highest probability occurs around $R(1000) = 0.903$. The high correlation coefficients obtained in the experiment show small intensity fluctuations of Φ -OTDR traces and high stability of sensor system, which is able to get vibration dynamic strain measurement with small uncertainty.

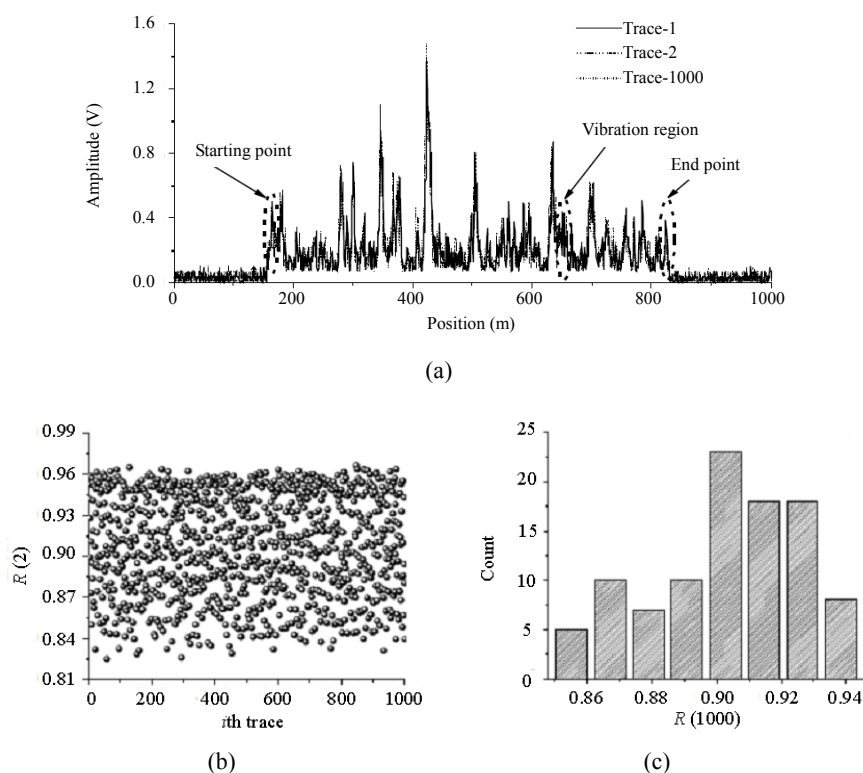


Fig. 4 Correlation coefficient analysis of Φ -OTDR traces: (a) the measured Φ -OTDR traces including a vibration region, (b) the distribution of $R(2)$ in one measurement with 1000 traces, and (c) the histogram distribution of calculated $R(1000)$ at non-vibration locations.

4. Vibration measurement

Φ -OTDR for vibration sensing can be simulated by calculating intensity at the vibration location based on (5), and its procedure is shown in Fig. 1. Figure 5(a) exhibits the first order and second order Bessel functions, $J_1(V_m)$ and $J_2(V_m)$, respectively. The data points of A, B, and C on the curve of the first order Bessel function correspond to those in Figs. 5(b), 5(c), and 5(d) which are simulated power spectra with $V_m = 0.25$ V, 1 V, and 2 V. Since the output of any order Bessel functions would change with different V_m , the vibration dynamic strain can thus be acquired by observing P_{vib} of the corresponding frequency in the power spectra. In Fig. 5(b), there is one peak at the vibration frequency $f_{\text{vib}} = 500$ Hz under the driving voltage of 0.25 V. According to (5), harmonics of higher orders in terms of Bessel functions remain and

become more and more noticeable for larger V_m values. Another peak at $2f_{\text{vib}}$ in Fig. 5(c) and even three other peaks at harmonic frequencies in Fig. 5(d) appear in the power spectra when V_m is further increased. The amplitudes of these peaks are determined by the magnitude of the second order and third order Bessel functions.

The above theoretical and simulation analysis indicates that the detection of V_m becomes available by monitoring relative peak magnitudes at the fundamental frequency and high-order harmonics, however, this work only demonstrates the case that the first order Bessel function plays a dominant role. The 500-Hz vibration event is identified at 490 m as shown in Fig. 6(a). Figures 6(b), 6(c), and 6(d) show the measured power spectra with different driving voltages of $V_m = 1.8$ V, 3 V, and 4 V.

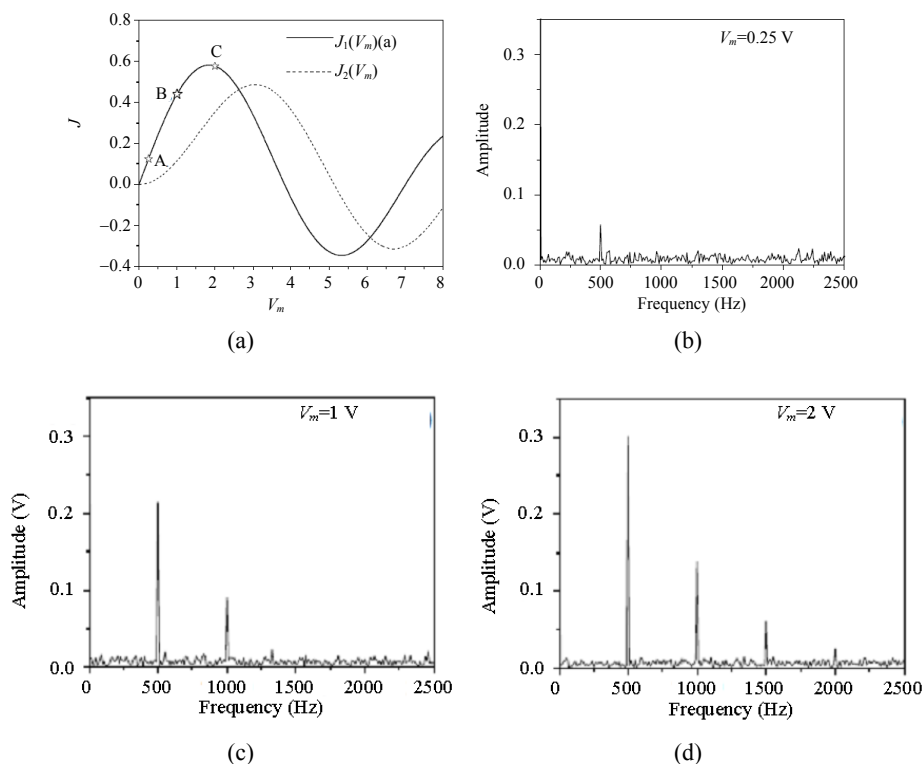


Fig. 5 Simulation results of vibration analysis: (a) the first order and second order Bessel functions. A, B, and C corresponds to those in Figs. 5(b), 5(c), and 5(d), respectively; simulation results of power spectra under different V_m : (b) $V_m = 0.25$ V, (c) $V_m = 1$ V, and (d) $V_m = 2$ V.

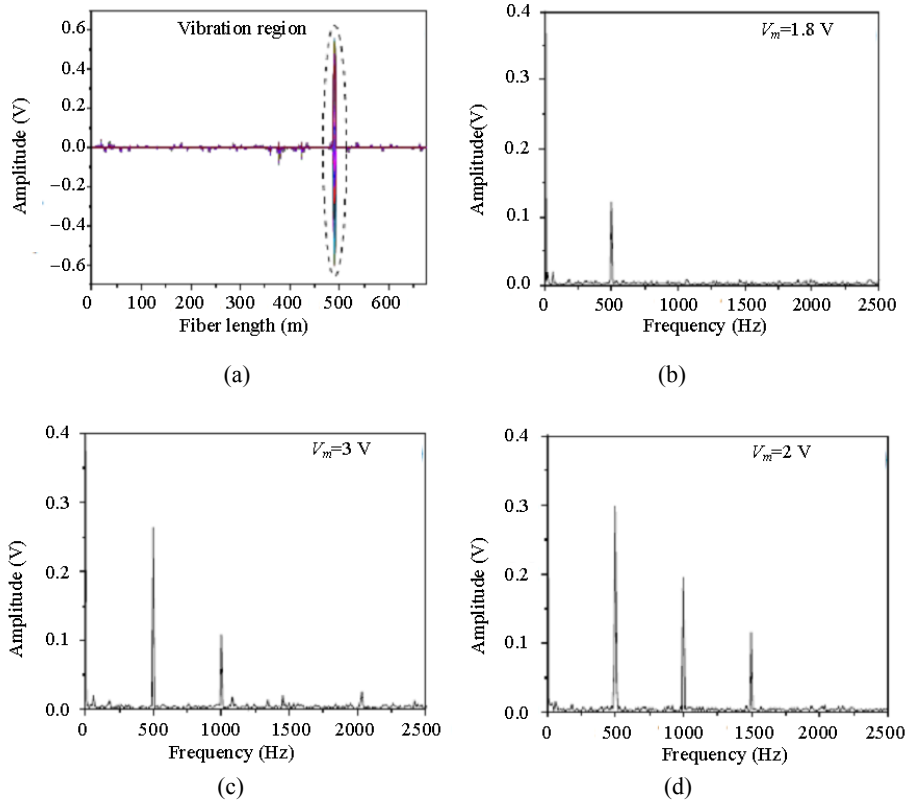


Fig. 6 Experimental results of vibration analysis: (a) vibration location information; experiment results of power spectra under different V_m : (b) $V_m = 1.8$ V, (c) $V_m = 3$ V, and (d) $V_m = 4$ V.

5. Measurement uncertainty analysis

In simulation, the applied vibration signal is modeled as a perfectly sinusoidal signal, and the system noise at the vibration region is assumed to be the same as that at other positions along the sensing fiber. Thus, the standard deviation of peak value σ_{vib} at the vibration frequency depends only on the system noise that can be characterized by the correlation coefficient $R(1000)$. Figure 7(a) shows the simulated σ_{vib} with varying R under $V_m = 0.25$ V, for 100 measurements. Figures 7(b) and 7(c) show the simulation and experimental results of σ_{vib} with different M under $V_m = 0.25$ V and $V_m = 2.2$ V, respectively. The Φ -OTDR system stability analysis at non-vibration locations has indicated that R_{nv} is about 0.9 corresponding to $F_{\text{nv}} = 0.004$. However,

the actual measured σ_{vib} [star dot in Fig. 7(c)] is much larger than the simulation result in Fig. 7(b1) and is comparable to the simulation result in Fig. 7(b2) when $F_v = 0.055$ and $R_v = 0.03$. An increase in F and a decrease in R imply that the fiber-wrapped PZT induces imperfect vibration signals and causes undesired phase changes which could further increase the measurement uncertainty of P_{vib} . In addition, σ_{vib} becomes smaller when a larger M is used for the spectrum analysis as shown in Fig. 7(c), and σ_{vib} is 0.0067 when $M = 1000$. This is because that the average random noise is approaching to the same level in each measurement when more traces are used. Thus, 1000 traces are selected in the experiment to achieve a small measurement uncertainty and a short measurement time.

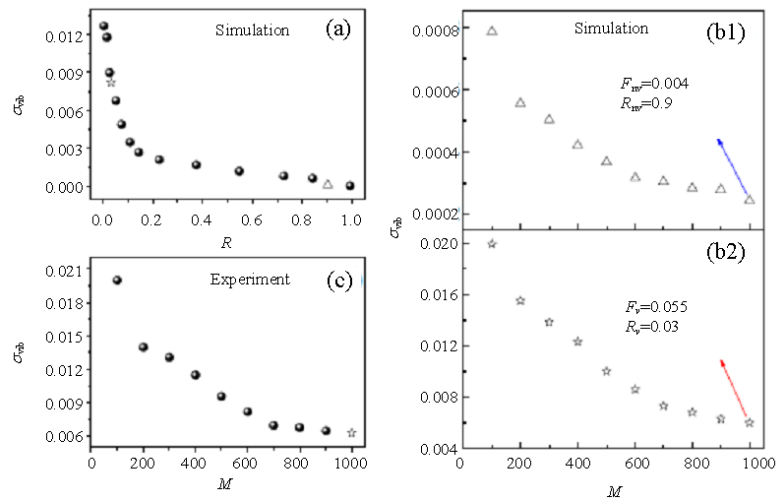


Fig. 7 Simulation result of σ_{vib} as a function of R : (a) and σ_{vib} as a function of M : (b) simulation and (c) experiment.

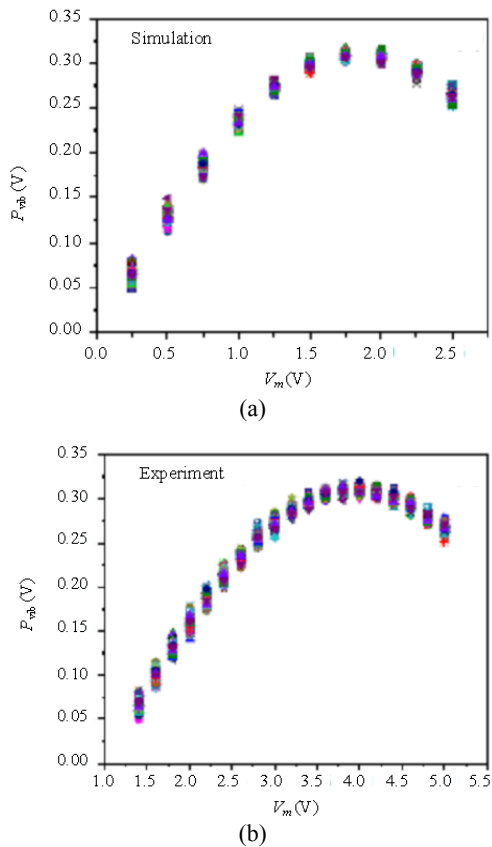


Fig. 8 Change in P_{vib} with different V_m : (a) simulation and (b) experiment.

Figure 8(a) shows the simulation result of P_{vib} with different V_m by using $F_v = 0.055$ and $M = 1000$ to match the experimental result as shown in Fig. 8(b). Both results are obtained with 100 measurements to guarantee reliable and repeatable measurements. The dynamic strain induced by

various driving voltages of PZT can be statistically extracted from the average value of P_{vib} . It should be noted that the measured V_m is the actual vibration amplitude of the sinusoidal vibration signal in the experimental result. The corresponding phase change induced by external vibration depends not only on V_m but also on the sensitivity coefficient η of PZT and fiber length wrapped on the PZT. Since our interest is the vibration strength, the simplified model is simulated by only considering V_m as the modulation depth to quantify the vibration amplitude which is an average value rather than a time dependent variable. This results in the different values of V_m between the simulation and experimental results. The experimental results show that the Φ -OTDR system has a high stability and low phase fluctuation because of high correlation coefficients and relative small measurement uncertainty obtained in the experimental results.

6. Conclusions

In conclusion, the high stability Φ -OTDR system has been successfully demonstrated for quantitative vibration measurements. The PZT vibration dynamic strain can be characterized by monitoring the peak values in the power spectra obtained by using the FFT of the time-domain waveform at the vibration location. The trace-to-trace correlation coefficient is introduced to

analyze the system noise, and it is also beneficial to the measurement uncertainty analysis. The experimental results demonstrate a good agreement with the simulation results.

Acknowledgment

M. Ren would also like to acknowledge the support from the NSERC CREATE: Sustainable Engineering in Remote Areas (SERA) program, and suggestion from Dr. D. P. Zhou. We like to acknowledge the supports from Canada Research Chairs; Natural Sciences and Engineering Research Council of Canada (NSERC).

Open Access This article is distributed under the terms of the Creative Commons Attribution 4.0 International License (<http://creativecommons.org/licenses/by/4.0/>), which permits unrestricted use, distribution, and reproduction in any medium, provided you give appropriate credit to the original author(s) and the source, provide a link to the Creative Commons license, and indicate if changes were made.

References

- [1] X. Bao and L. Chen, "Recent progress in Brillouin scattering based fiber sensors," *Sensors*, 2011, 11(4): 4152–4187.
- [2] M. A. Soto, G. Bolognini, and F. D. Pasquale, "Enhanced simultaneous distributed strain and temperature fiber sensor employing spontaneous Brillouin scattering and optical pulse coding," *IEEE Photonics Technology Letter*, 2009, 21(7): 450–452.
- [3] B. Soller, D. Gifford, M. Wolfe, and M. Foggatt, "High resolution optical frequency domain reflectometry for characterization of components and assemblies," *Optics Express*, 2005, 13(2): 666–674.
- [4] D. Zhou, Z. Qin, W. Li, L. Chen, and X. Bao, "Distributed vibration sensing with time-resolved optical frequency-domain reflectometry," *Optics Express*, 2012, 20(12): 13138–13145.
- [5] Q. Cui, S. Pamukcu, W. Xiao, and M. Pervizpour, "Truly distributed fiber vibration sensor using pulse base BOTDA with wide dynamic range," *IEEE Photonics Technology Letter*, 2011, 23(24): 1887–1889.
- [6] J. C. Juarez, E. W. Maier, K. N. Choi, and H. F. Taylor, "Distributed fiber-optic intrusion sensor system," *Journal of Lightwave Technology*, 2005, 23(6): 2081–2087.
- [7] J. C. Juarez and H. F. Taylor, "Field test of a distributed fiber-optic intrusion sensor system for long perimeters," *Applied Optics*, 2007, 46(11): 1968–1971.
- [8] F. Peng, H. Wu, X. Jia, Y. Rao, Z. Wang, and Z. Peng, "Ultra-long high-sensitivity Φ -OTDR for high spatial resolution intrusion detection of pipelines," *Optics Express*, 2014, 22(11): 13804–13810.
- [9] Y. Lu, T. Zhu, L. Chen, and X. Bao, "Distributed vibration sensor based on coherent detection of phase-OTDR," *Journal of Lightwave Technology*, 2010, 28(22): 3243–3249.
- [10] Z. Qin, L. Chen, and X. Bao, "Wavelet denoising method for improving detection performance of distributed vibration sensor," *IEEE Photonics Technology Letter*, 2012, 24(7): 542–544.
- [11] T. Zhu, Q. He, X. Xiao, and X. Bao, "Modulated pulses based distributed vibration sensing with high frequency response and spatial resolution," *Optics Express*, 2013, 21(3): 2953–2963.
- [12] G. Tu, X. Zhang, Y. Zhang, F. Zhu, L. Xia, and B. Nakarmi, "The development of Φ -OTDR system for quantitative vibration measurement," *IEEE Photonics Technology Letter*, 2015, 27(12): 1349–1352.
- [13] A. Masoudi, M. Belal, and T. P. Newson, "A distributed optical fibre dynamic strain sensor based on phase-OTDR," *Measurement Science and Technology*, 2013, 24(8): 085204.
- [14] P. Healey, "Fading in heterodyne OTDR," *Electronics Letters*, 1984, 20(1): 30–32.
- [15] H. Izumita, S. Furukawa, Y. Koyamada, and I. Sankawa, "Fading noise reduction in coherent OTDR," *IEEE Photonics Technology Letter*, 1992, 4(2): 201–203.
- [16] H. Izumita, Y. Koyamada, S. Furukawa, and I. Sankawa, "Stochastic amplitude fluctuation in coherent OTDR and a new technique for its reduction by stimulating synchronous optical frequency hopping," *Journal of Lightwave Technology*, 1997, 15(2): 267–278.
- [17] A. K. Wojcik, "Signal statistics of phase dependent optical time domain reflectometry," Ph.D. dissertation, Texas A & M University, College Station, TX, USA, 2006.